

# 100th Anniversary of Macromolecular Science Viewpoint: Macromolecular Materials for Additive Manufacturing

Benjaporn Narupai and Alshakim Nelson\*



Cite This: *ACS Macro Lett.* 2020, 9, 627–638



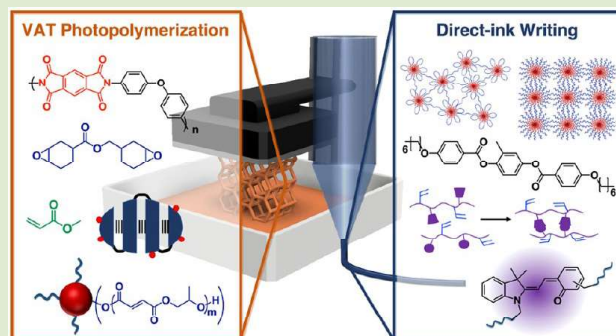
Read Online

ACCESS |

Metrics & More

Article Recommendations

**ABSTRACT:** Additive manufacturing (AM) has drawn tremendous attention as a versatile platform for the on-demand fabrication of objects with excellent spatial control of chemical compositions and complex architectures. The development of materials that are specifically designed for AM is highly desirable for a variety of applications ranging from personal healthcare, tissue engineering, biomedical devices, self-folding origami structures, and soft robotics. Polymeric macromolecules have received increasing attention due to a wide variety of materials, the versatility for novel chemistries, and the ability to tune chemical composition and architecture. This Viewpoint highlights the development of polymeric materials for direct-ink writing and vat photopolymerization for 3D printing applications. Recent chemical innovations and polymer architectures are overviewed, which also includes recent developments in responsive and adaptive objects from AM. Polymers for biological interface and sustainability in AM are also discussed.



The field of polymer science has developed at an amazing pace since it was first defined 100 years ago by Hermann Staudinger.<sup>1</sup> Polymers are now a mainstay in our society that are used for a broad range of applications in consumer goods, healthcare, and aerospace/automotive industries. At the same time, we have witnessed the rapid progression of digital tools and technologies, the first digital computer was ENIAC in 1946, and computers have become equally pervasive. Additive manufacturing (AM) lies at the interface between these two fields, wherein 3D printing hardware is combined with computer software/modeling and a host of polymeric and nonpolymeric materials (Figure 1). Advanced manufacturing processes such as AM present a huge opportunity for the polymer community to develop materials designed for AM that create functional 3D objects and meet the physicochemical prerequisites for its use in existing and emerging applications.

A wide variety of AM hardware is available, all of which rely on a layer-by-layer or continuous deposition of a material to fabricate 3D objects.<sup>2</sup> Material extrusion printing, stereolithographic apparatus (SLA) printing, and selective laser sintering are the most common methods to 3D print polymeric materials.<sup>3</sup> Detailed descriptions of these techniques will be omitted here since many reviews are available.<sup>4–9</sup> The two most common forms of material extrusion are fused deposition modeling (FDM) and direct-ink writing (DIW). Both processes involve the extrusion of a material through a nozzle onto a build platform. While FDM primarily uses a heated nozzle to extrude a thermoplastic filament, DIW requires inks whose viscoelastic

properties enable extrusion when placed under a mechanical or pneumatic load. Shear-thinning inks with viscosities that decrease with applied shear rates are preferred for DIW. These viscoelastic polymer inks flow under high-strain conditions, but then cease to flow under low-strain conditions. SLA printing is highly attractive for its production speed and resolution. As a light-based process, it is highly amenable to a range of photopolymerization chemistries.<sup>10,11</sup>

This Viewpoint will highlight some of the recent developments in polymeric materials for AM using DIW and SLA processes. These two techniques have witnessed the most development with respect to new polymer materials over the last several years. For both these techniques, the viscoelastic properties of the ink or resin and the cross-linking chemistries utilized are of utmost importance. These parameters are controlled based on many of the fundamental principles of polymer chemistry: polymer- and network-forming reactions, composition, molecular weight, and polymer architecture are just some of the means by which new polymeric materials for

Received: March 8, 2020

Accepted: April 10, 2020

Published: April 15, 2020



ACS Publications

© 2020 American Chemical Society

## Additive Manufacturing

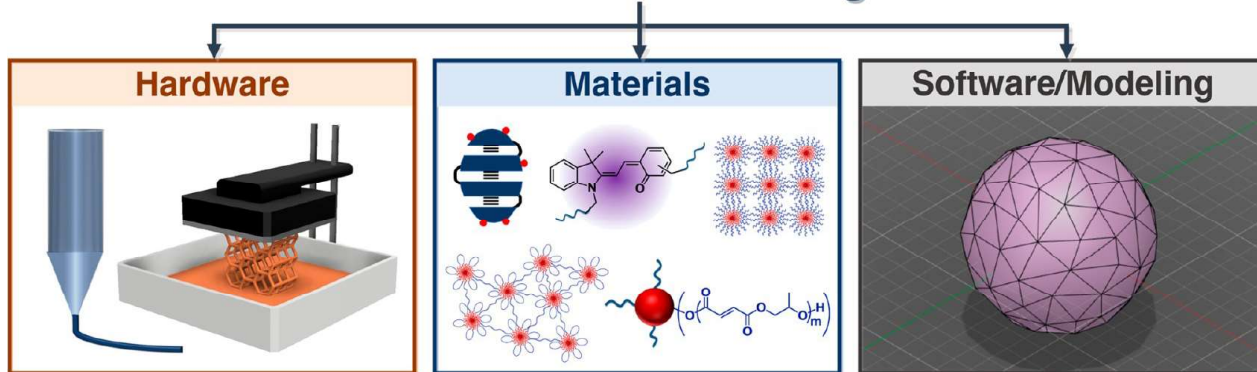


**Figure 1.** Additive manufacturing requires (1) hardware, such as an extrusion-based 3D printer, stereolithographic 3D printer, (2) materials including polymeric and nonpolymeric materials, and (3) computer software/modeling, such as computer-aided design (CAD) and image processing.

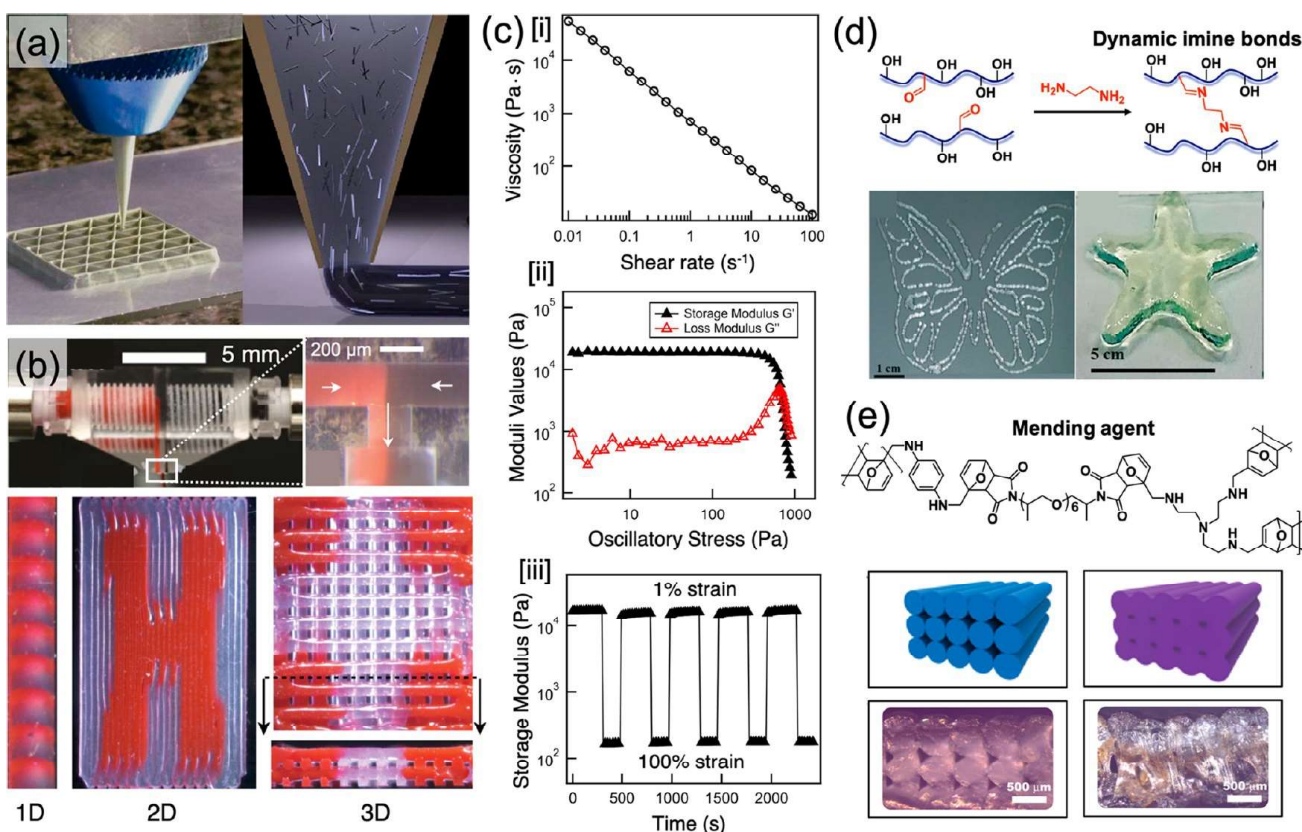


**Figure 2.** (a) An example of direct-ink writing (DIW; Reproduced with permission from ref 12. Copyright 2014 Wiley-VCH). (b) A nozzle with two independently actuated syringe pumps and printed multimaterial structures of 1D extruded filament, a 2D "H" pattern and a 3D four-layer log pile structure (Reproduced with permission from ref 20. Copyright 2015 Wiley-VCH). (c) Rheological experiments: [i] viscosity vs shear rate profile demonstrating shear thinning properties, [ii] strain sweep representing the yielding point in response to applied stress, and [iii] cyclic shear-thinning experiment illustrating storage modulus response and instantaneous recovery to alternating low (1%) and high (100%) strains (Reproduced with permission from ref 14. Copyright 2019 Wiley-VCH). (d) The synthesis of poly(hydroxyethyl methacrylate) (PHEMA) with pendant benzaldehyde groups, followed by a cross-linking with a diamine and 3D printed structures (Reproduced with permission from ref 23. Copyright 2017 Royal Society of Chemistry). (e) Structure and composition of the reversible Diel-Alder mending agent for FDM. Illustration of 3D printed PLA filaments (blue) and PLA blended with mending agent (purple) and their corresponding microscopic images (Reproduced with permission from ref 24. Copyright 2016 American Chemical Society).

AM have been developed. The recent implementation of these concepts to advance the field of AM will be presented.

**New chemistries for material extrusion printing:** There are two strategies to print inks via a direct-write process. In the first

approach, a low viscosity ink is extruded from a nozzle and is chemically, photochemically, or noncovalently cross-linked during or immediately after extrusion. For example, calcium alginate gels have been printed in this manner using divalent

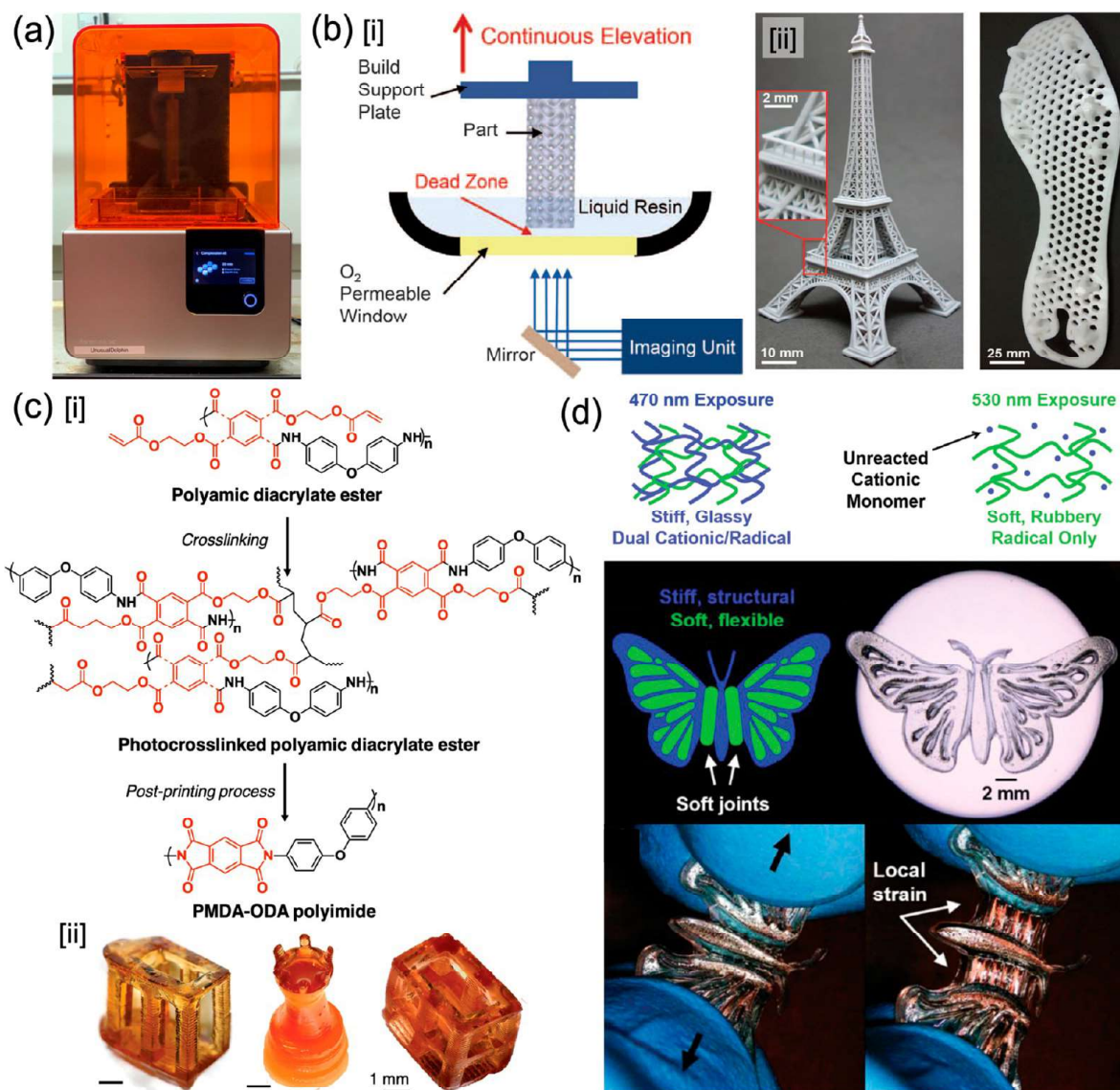


**Figure 3.** (a) A commercially available (Form 2) printer for vat photopolymerization via a scanning laser-based process. (b) [i] Schematic of CLIP printer where the oxygen-permeable window creates a dead zone between the elevating part and the window; [ii] Eiffel Tower model and a shoe cleat can be fabricated using CLIP (Reproduced with permission from ref 25. Copyright 2015 The American Association for the Advancement of Science). (c) [i] Molecular structure of photo-cross-linkable polyamic diacrylate ester precursor polymer, polymer after cross-linking process, and PMDA-ODA polyimide after postprinting process; [ii] Images of anisotropic 3D structures after printing using mask-projection microstereolithography (MP $\mu$ SL; Reproduced with permission from ref 38. Copyright 2017 Wiley-VCH). (d) Schematic of network structure of the resin combination using blue exposure for dual radical and cation curing while green exposure for only radical cross-linking and the 3D printed butterfly with stiff sections and soft joints (Reproduced with permission from ref 40. Copyright 2018 Wiley-VCH).

calcium ions to the carboxylate functionalities of the polysaccharide. Alternatively, a shear-thinning ink that exhibits a viscoelastic response to applied pressure can be extruded from a nozzle to directly deposit the ink to fabricate a 3D object (Figure 2a).<sup>12</sup>

DIW is the most versatile form of AM and inks based on hydrogels,<sup>13</sup> ionogels,<sup>14</sup> silicones,<sup>15</sup> and polymer nanocomposites<sup>16–18</sup> have been developed. The functionality of these materials are readily tuned with additives that make this AM approach attractive from the standpoint of developing new materials. DIW also readily enables multimaterial printing using two or more nozzles to afford more complex 3D objects. One of the biggest challenges in the AM field is the fabrication of spatially defined multimaterial 3D printed objects. Extrusion-

based processes are best suited for multimaterial printing because each material can be independently deposited in a patternwise manner for each layer of the object.<sup>19</sup> Commercially available extrusion and FDM have the capability to afford multicolored objects, and Lewis and co-workers have demonstrated microfluidic printheads for the multimaterial 3D printing (Figure 2b).<sup>20</sup>

In general, shear-thinning inks are desired for DIW printing (Figure 2c). There have been several reports that have aimed to quantify the viscoelastic properties required for DIW inks,<sup>21,22</sup> but a universal set of parameters has yet to emerge. As a result, the development of new inks is largely based on trial and error, which requires the viscoelastic properties of the ink (primarily shear-thinning behavior (Figure 2c[i]) and yield stress (Figure

2c[ii])) to be optimized along with hardware parameters such as translational print speed, nozzle height, and nozzle diameter. Polymeric inks that are designed to be shear-thinning should also exhibit rapid recovery of the gel state as well (Figure 2c[iii]). Thus, many of these materials are physically cross-linked via polymer phase separation or ionic cross-linking. Examples of these materials will be provided in this Viewpoint.

Dynamic covalent bonds exhibit a reversible character that can be utilized to afford materials that can be extruded through a nozzle or needle. Many of these materials are hydrogels that have been developed for subdermal delivery, but there are still relatively few reports of successful material extrusion 3D printing. Connal and co-workers demonstrated an imine-based organogel prepared from benzaldehyde-functionalized poly(2-hydroxyethyl methacrylate) (PHEMA) and ethylenediamine (Figure 2d).<sup>23</sup> These gels were shear-thinning and self-healing and were extrusion printed to form self-healing objects. The reversibility of the imine bonds enabled the material to be extruded while these covalent bonds were broken, and then rapidly regain its gel state as the imine bonds were reformed. As another example of utilizing reversible covalent bonds, the reversibility of Diels–Alder chemistry was used to facilitate self-healing of filament defects introduced during FDM printing of poly(lactic acid) (PLA; Figure 2e).<sup>24</sup> The thermal reversibility of Diels–Alder adducts was advantageous during the extrusion of the PLA filament to allow the thermoplastic composite to flow during melt extrusion. Upon cooling, the furan and maleimide functionalities reformed the adduct to ultimately improve the adhesion between the extruded layers, as well as the mechanical properties of the PLA composite.

New chemistries for vat photopolymerization printing: SLA processes (based on laser-scanning or digital projection) are attractive because they can provide more complex geometries relative to DIW at much higher rates of production (Figure 3a). DeSimone and co-workers ignited the polymer field with the first report of continuous liquid interface production (CLIP) of 3D objects (Figure 3b).<sup>25</sup> This AM technique uses an oxygen-permeable window through which patterned light is projected. The presence of oxygen at this interface produces a zone of inhibition between the polymerizing part and the window where photopolymerization is prevented (Figure 3b[i]). As a result, complex 3D objects can be printed in the span of minutes (Figure 3b[ii]). In this seminal example, the critical advancement in the hardware for AM was strongly coupled to an understanding of the chemical process.

The CLIP technology not only spawned a company (Carbon), but also inspired further developments in the field with a strong coupling of AM hardware with chemistry and materials science. For example, Burns, Scott, and co-workers developed an approach that does not require oxygen permeable windows that produce the zone of oxygen inhibition.<sup>26</sup> They demonstrated a continuous stereolithographic printing process wherein simultaneous two-color irradiation independently activated a photoinitiator for patternwise polymerization of the resin and a photoinhibitor to spatially confine photopolymerization and produce a zone of inhibition. In addition to the rapid speed of production, this dual-wavelength technique enabled localized surface patterning of features for the first time. In another example of coupling AM hardware with chemistry, Moore and White utilized the frontal polymerization of ring-opening metathesis polymerization to afford intricate 3D printed thermosets that was fully cured within seconds.<sup>27</sup> A thorough understanding of the polymerization kinetics and heat

generated during the reaction was pertinent to this unique method of printing.

Improvements in spatiotemporal control over the chemical cross-linking is required to improve the performance of vat photopolymerization techniques. Wong and co-workers recently introduced a strategy of cross-linking the carboxylate groups of alginate chains using a caged divalent metal ions.<sup>28</sup> A photoacid generator (diphenyliodonium nitrate) was used to uncage Mg<sup>2+</sup>, Ca<sup>2+</sup>, or Ba<sup>2+</sup> dication from their respective salt complexes. AM requires the ability to chemically cross-link a material rapidly on demand. This strategy introduces one method by which a “caging” approach was effective for spatiotemporal control over a cross-linking reaction, and a similar strategy with other chemical systems may prove to be equally effective.

Vat photopolymerization using new polymerization methodologies based on RAFT<sup>29</sup> or thiol–ene coupling,<sup>30</sup> and new chemical compositions of polymers are also emerging in the field.<sup>31–37</sup> Engineering polymers are highly desirable for aerospace and automotive applications as a consequence of their mechanical properties and thermal stability at high temperatures. However, these highly aromatic materials can already be difficult to process and manipulate using traditional methods. Long and co-workers recently reported a strategy to produce an all-aromatic polyimide via SLA printing.<sup>38</sup> In this approach, a soluble poly(amic ester) precursor containing photo-cross-linkable acrylate groups was synthesized (Figure 3c[i]). This precursor undergoes light-induced chemical cross-linking using mask projection microstereolithography (MPμSL) affording 3D objects (Figure 3c[ii]). Then, controlled solvent removal and postprinting thermal imidization were performed to transform the cross-linked 3D organogel to the thermoplastic pyromellitic dianhydride and 4,4'-oxidianiline (PMDA-ODA) polyimide (Figure 3c[i]). This strategy is exemplary of the types of chemical strategies that can be used to produce high-performance parts with excellent thermal stability for demanding applications.

Vat photopolymerization techniques typically use a single resin vat that contains polymerizable resin formulation. Gray scale printing with a single resin has been demonstrated,<sup>39</sup> but multimaterial objects from vat photopolymerization processes is an ongoing challenge. The speed of production in a vat photopolymerization process is drastically reduced if the resin composition must be changed during the printing process. Recent developments using orthogonal chemistries within a single resin are a promising approach to address this challenge.

Hawker and co-workers demonstrated spatially controlled multimaterial 3D printed objects using an approach termed solution mask liquid lithography (SMaLL).<sup>40</sup> This process utilized the initiation of two different polymerization chemistries: radical polymerization versus the combined radical and cationic polymerization) using 530 and 470 nm visible light, respectively, from a multimaterial resin mixture (Figure 3d). Around the same time, Boydston and co-workers demonstrated an example of multimaterial vat photopolymerization using similar orthogonal chemistries initiated by two different wavelengths of light.<sup>41</sup> In both of these reports, the monomers present in the resin were chosen such that the acrylates afforded soft elastomeric domains, while the combination of polymerized acrylates and epoxy monomers afforded stiff networks. The spatial control over chemical heterogeneity and mechanical anisotropy was successfully employed to produce 3D objects with soft and stiff regions that could be used to afford shape-changing constructs<sup>41</sup> (4D printing) from a single vat of resin.

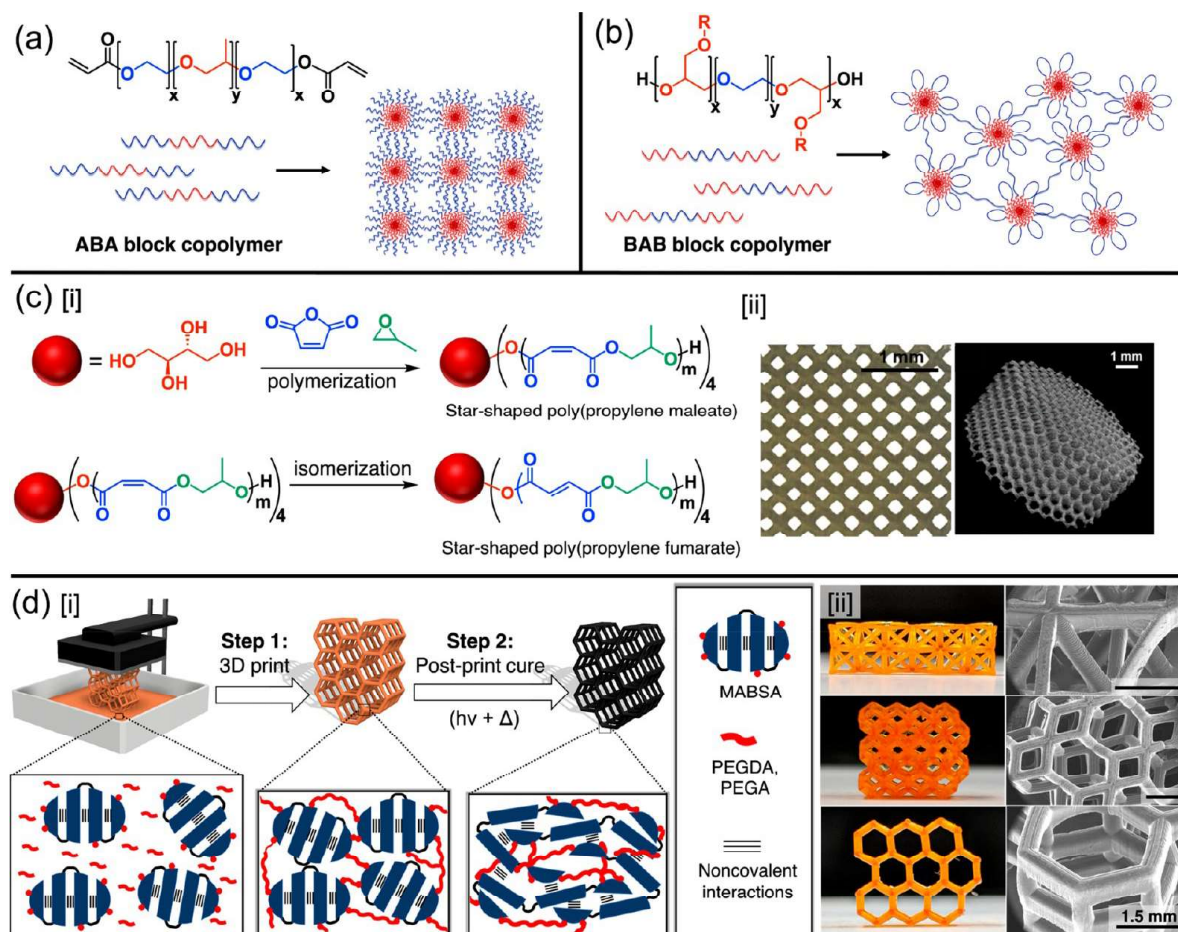


**Figure 4.** (a) Poly(ethylene oxide)-*b*-poly(propylene oxide)-*b*-poly(ethylene oxide) triblock copolymer (ABA) after acylation and cartoon representation of micelles formation in water that pack into packed latices. (b) Poly(alkyl glycidyl ether)-*b*-poly(ethylene glycol)-*b*-poly(alkyl glycidyl ether) triblock copolymer (BAB) and cartoon representation of flower-like micelles formation. (c) [i] Synthesis of star-shaped poly(propylene maleate) and subsequent isomerization into star-shaped poly(propylene fumarate); [ii] Optical microscopy image and  $\mu$ -CT image of a 3D printed gyroidal scaffold (Reproduced with permission from ref 50. Copyright 2019 Royal Society of Chemistry). (d) [i] The two-step process to fabricate protein-based bioplastics using vat photopolymerization; [ii] Optical and SEM images of 3D printed lattice structures (Reproduced with permission from ref 51. Copyright 2020 American Chemical Society).

Polymer architecture in material extrusion printing: An infinite array of acrylate and methacrylate-based formulations are possible as resins for AM, and the choice of monomer ultimately affects the mechanical properties of the printed part. However, over the last several decades, the polymer field has developed a range of polymer architectures including block copolymers, graft copolymers, star polymers, hyperbranched polymers, etc. that have a significant impact on the viscoelastic characteristics of inks and resins for additive manufacturing. For example, F127 is a commercially available triblock copolymer of poly(ethylene oxide)-*b*-poly(propylene oxide)-*b*-poly(ethylene oxide) that affords shear-thinning hydrogel inks for extrusion-based printing. The triblock copolymer forms micelles in water that pack into packed latices at the appropriate concentrations (Figure 4a). The micelles are believed to slide past one another while the gel is shear-thinning. The F127 hydrogels have been used as support or sacrificial constructs during a printing process, but meth(acrylated) forms of this polymer afford a hydrogel ink that can be extrusion printed and subsequently UV-cured to afford cross-linked gel networks.<sup>42</sup>

One of the limitations of F127 is the concentration of polymer required to have an extrusion printable hydrogel (typically >25

wt %). Whereas F127 is an ABA triblock copolymer in which hydrophilic “A” blocks flank a central “B” block, our group has explored a BAB triblock copolymer architecture (Figure 4b).<sup>43,44</sup> These micelles self-assemble to form flower-like micelles that can form shear-thinning hydrogels for extrusion-based 3D printing. Interestingly, these polymers gel in water at concentrations that are lower than F127 polymers (10 wt %). This is attributed to the polymer architecture, as the BAB triblock configuration is known to form flower micelles with polymers that can span between two micelles to create a network of physically cross-linked micelles.

The Heise and in het Panhuit groups also investigated the effect of architecture on printable inks using star polymers comprised of an amphiphilic block copolymer structure of poly(benzyl-L-glutamate)-*b*-oligo(L-valine) polymerized from a poly(propyleneimine) dendrimer.<sup>45</sup> These roughly spherical polymers bear a structural resemblance to the F127 micelles and have the effect of affording shear-thinning gels that can rapidly recover its gel state after extrusion. In this case, the hydrogen bonding interactions between the star polymers were proposed to be responsible for the gelation.

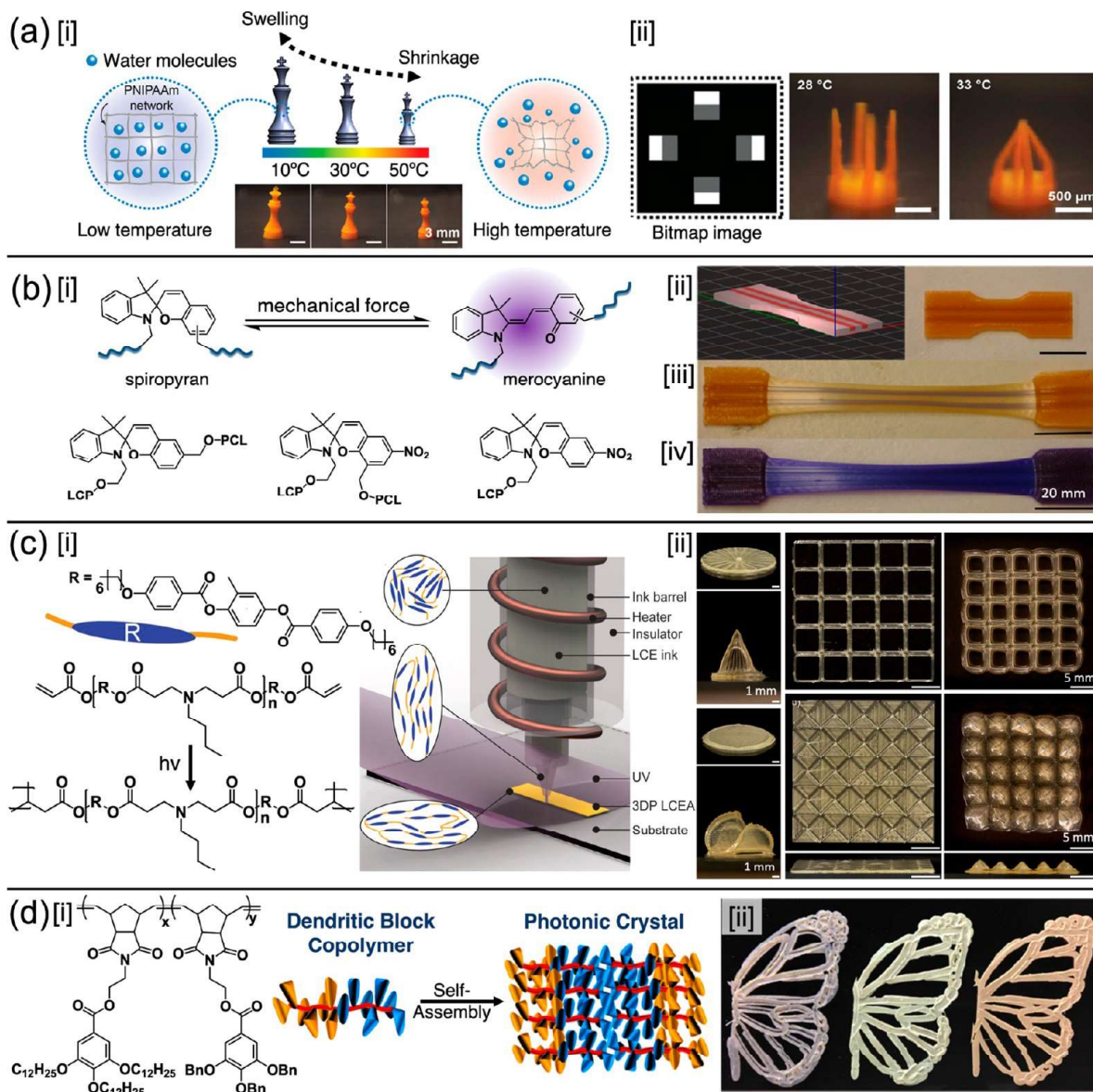


**Figure 5.** (a) [i] Temperature-responsive swelling of 3D printed poly(*N*-isopropylacrylamide) (PNIPAAm) hydrogel structure using projection microstereolithography (P $\mu$ SL); [ii] A 3D printed gripper with four beams fabricated using two different grayscale levels. The beams bend toward the center at high temperature due to different swelling ratio between the two regions. (b) [i] The mechanochemical isomerization of a spiropyran moiety to its merocyanine form and chemical structure of three spiropyran-containing poly(caprolactone) (PCL), [ii] test specimen pre-elongation with red stripes, indicating the location of mechano-responsive material, [iii] test specimen post-elongation, demonstrating the mechanochromic response, and [iv] test specimen post-elongation after 365 nm UV irradiation (Reproduced with permission from ref 58. Copyright 2015 American Chemical Society). (c) [i] The photopolymerizable liquid crystal elastomer (LCE) and schematic illustration of high operating temperature direct-ink writing (HOT-DIW) showing ordered LCE ink morphology due to induced director alignment within the nozzle; [ii] Programmable shape morphing liquid crystal elastomer actuators upon heating above their nematic–isotropic transition temperature (Reproduced with permission from ref 64. Copyright 2018 Wiley-VCH). (d) [i] Chemical structure of rigid-rod dendritic block copolymer and schematic representation of self-assembly of block copolymer to photonic crystal; [ii] Photograph of a 3D-printed butterfly wing reflecting violet, green, and red light (Reproduced with permission from ref 65. Copyright 2017 American Chemical Society).

Supramolecular and mechanically interlocked macromolecules also represent an intriguing molecular architecture for printing 3D objects. Ke and co-workers developed 3D printed polypseudorotaxane-based hydrogels which consisted of  $\alpha$ -cyclodextrins threaded onto F127. After postprinting polymerization, the motion of the  $\alpha$ -cyclodextrin rings can switch between random shuttling and stationary states by solvent exchange, resulting in reversible deformation and reformation to its 3D structure.<sup>46,47</sup>

Polymer architecture in vat photopolymerization printing: Generally, the design of new oligomers and polymers for vat photopolymerization is challenged by the increase in viscosity of the resin with polymer concentration and molecular weight, as predicted by the Mark–Houwink equation. Resins that exhibit a high viscosity ( $>10$  Pa·s)<sup>48,49</sup> are slow to self-level and exert greater capillary forces that hamper vat photopolymerization. An alternative design strategy is to employ polymer architectures such as cyclic, branched, dendritic, or cross-linked unimolecular

particles architecture that have a lower intrinsic viscosity relative to a linear polymer of comparable molecular weight.

Becker and co-workers reported the first example of using polymer architecture to affect the viscosity of resins for vat photopolymerization.<sup>50</sup> Four-arm star polymers with a narrow molar mass range were synthesized via ring-opening copolymerization of maleic anhydride and propylene oxide followed by isomerization of the alkene to afford the corresponding poly(propylene fumarate) (Figure 4c[i]). Resins formulated from four-arm star polymers had viscosities that were lower than the corresponding linear polymers of comparable molecular weight. This result is important because prior to this development, linear polymers with a degree of polymerization (DP) > 20 were challenging to print as a consequence of their increased viscosity. The star polymer architecture afforded polymers with a DP as high as 200, which could be 3D printed as gyroid lattices using a DLP printer (Figure 4c[ii]). These resins were photocured in the presence of a photoradical generator to polymerized the alkenes of the fumarate functionalities. Another advantage of this polymer platform is the biodegradability of the polyester arms of the star polymer. The star polymer architecture now enables the study of molecular weight and star architecture on the mechanical properties and degradation characteristics of these materials.

Our group has recently shown that globular proteins, such as methacrylated bovine serum albumin (MABSA), also possess an ideal architecture suitable for vat photopolymerization (Figure 4d[i]).<sup>51</sup> BSA is a soluble globular protein that is a single polypeptide (macromolecular) chain folded into a globular nanoparticle. Despite the high molecular weight of the protein, ~66 kDa, MABSA has excellent solubility in water (up to ~40% w/v) as a consequence of its compact three-dimensional shape and negatively charged surface.<sup>37</sup> Furthermore, the viscosity of these aqueous solutions changes minimally up to 35 wt % of protein. The protein was formulated to afford low viscosity resins for 3D printing of protein-based hydrogel constructs using a commercially available Form 2 printer. After a postprint thermal cure that denatured the proteins, the 3D printed bioplastics exhibited excellent mechanical properties, with tensile and compressive moduli comparable to polylactide (PLA; Figure 4d[ii]).

**Responsive and adaptive objects from AM:** Additive manufacturing presents an opportunity to create 3D objects that can respond and engage in more than one dimension. Stimuli-responsive materials in AM have great potential for applications in actuators or sensors used in soft robotics or in the medical field. Soft robots that can replicate the types of movement observed in nature may require the design and material complexity that only AM can offer in the future.<sup>52</sup> Stimuli-responsive polymeric materials that can respond to environmental cues such as pH, temperature, mechanical forces, and light will serve an important role in the future of AM.

**Temperature- and pH-responsive materials:** Poly(*N*-isopropylacrylamide) (PNIPAM) is a polymer that is well-known to possess a lower critical solution temperature (LCST, typically 32–35 °C) at which the polymer undergoes a coil-to-globule change in water.<sup>54</sup> As a result, the polymer chains undergo a significant volume and solubility change, which can be used to incorporate thermally induced stimuli-responsive behaviors in 3D printed objects.<sup>55</sup> Lee and co-workers used DLP SLA printing to fabricate PNIPAM-containing hydrogels that exhibited reversible temperature-dependent deformations (Figure 5a[i]).<sup>56</sup> Interestingly, the shape-change response was tuned

based on the composition and the layer height during the printing process. The former altered the temperature at which the response occurred, while the latter was used to control the anisotropic swelling (lateral vs vertical) in the object (Figure 5a[ii]). Monomers that are inherently pH-sensitive have been employed to create pH-responsive 3D printed objects. Cohn and co-workers demonstrated that F127 functionalized at its chain ends with methacrylate functionalities could be coformulated with acrylic acid (AA) in water to afford resins for vat photopolymerization.<sup>57</sup> As expected, these resins could be used to create pH-responsive objects that changed its degree of swelling in water. At pH 2.0, the AA groups were protonated and could participate in hydrogen-bonding interactions that limited the water uptake by the hydrogel. Above pH 5.0, the AA groups became ionized, and the water uptake was significantly higher due to electrostatic osmosis induced by the charged AA moieties.

**Mechanochemistry in additive manufacturing:** Mechano-phores are molecules that transform mechanical forces into a chemical response. The incorporation of these modalities into polymeric materials has emerged as a burgeoning field of research over the past decade. Boydston and co-workers first reported a mechanoactive 3D printed construct in which spirocyclic-containing poly(caprolactone) was extrusion printed using a filament extrusion printer (Figure 5b[i]).<sup>58</sup> 3D printed dogbones exhibited a color change from yellowish to blue/purple as the spirocyclic was ring-opened in response to a tensile load (Figure 5b[ii–iv]). These polymers were synthesized via ring-opening polymerization of caprolactone from a spirocyclic diol to afford linear polymers with a single mechanochrome at its center. Other examples of 3D printed polymeric mechanophores as more complex geometrical objects with a broader range of mechanical properties have emerged since this seminal paper.<sup>59,60</sup>

**Shape-morphing materials:** There are many examples of 3D printed objects that can change shape or actuate reversibly over time (often referred to as 4D printing).<sup>61–63</sup> One of the challenges associated with this field are shape-changing constructs with short actuation times. Moreover, many shape-morphing materials are hydrogels, which may limit their utility in nonaqueous environments. A notable recent example that circumvents these challenges used a liquid crystalline polymer to produce a reversible temperature-responsive actuator. Liquid crystal elastomers are polymeric materials that are capable of reversible shape changes in response to external stimuli such as temperature, light, or an electric field. Lewis and co-workers used a thermal extrusion-based 3D printing method to align photopolymerizable main-chain liquid crystal elastomeric inks in the direction of the print path (Figure 5c[i]).<sup>64</sup> As a result, the alignment of the mesogen domains afforded 3D printed objects that served as actuators. The shear-induced alignment of the mesogens was particularly advantageous in the case to maximize the anisotropy of the system. As a result, the 3D printed constructs actuated when heated above their nematic–isotropic transition temperature and could lift more weight than other liquid crystal elastomer actuators to date (Figure 5c[ii]).

**Light-responsive materials:** Temperature-induced self-assembly can be used to create well-defined nanostructures in thermoplastics. For example, a recent innovation in temperature-responsive filaments for FDM printing is the use of thermoplastic dendritic block copolymers as 3D printed photonic crystals.<sup>65</sup> Ring-opening metathesis polymerization (ROMP) of dendronized norbornene monomers afforded rigid

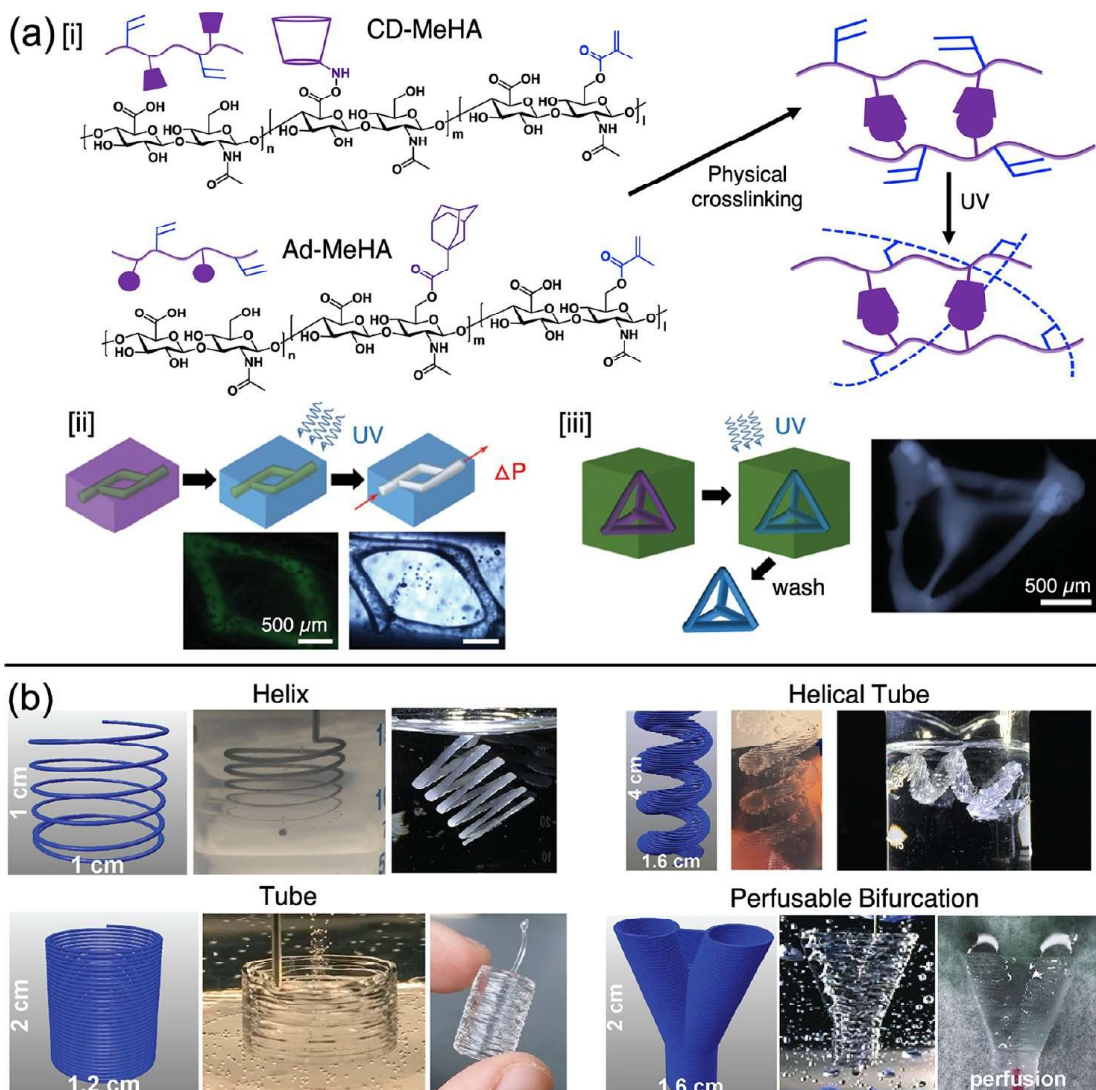


**Figure 6.** (a) [i] Hyaluronic acid modified with both methacrylates and host and guest molecules. These macromers cross-link by both physical bonding upon mixing and a secondary cross-linking of methacrylates after UV light irradiation; [ii] The printing of channels by writing an ink into a support gel which is modified for UV irradiation covalently cross-links; [iii] The printing of self-supporting structures by writing an ink that can be cross-linked into a support gel (Reproduced with permission from ref 74. Copyright 2015 Wiley-VCH). (b) 3D printed PDMS helix, tube, helical tube and perfusible bifurcation using Carbopol support (G-code of printed structures, printed structures embedded in Carbopol gel, and printed structures after curing and release; Reproduced with permission from ref 78. Copyright 2016 American Chemical Society).

rod block copolymers that self-assembled into ordered nanostructures that could be tuned to reflect light across the visible spectrum (Figure 5d[i]). The as-synthesized macromolecules, with a weight-average molecular weight of 484 kDa and  $D = 1.10$ , were colorless due to the absence of ordered, nanostructured periodicity. However, the melt-extruded filament (200 °C) was demonstrated to self-assemble during the extrusion process to afford a printed construct that could reflect violet light. The reflected and transmitted color (violet, green, or red) was dependent on the molecular weight of the polymer (Figure 5d[ii]). These novel materials can potentially be developed into optical filters and waveguides. Other light-responsive materials can also undergo shape changes in response to light. Genzer and co-workers demonstrated a simple strategy to create sequential self-folding of 2D polymer sheets into 3D objects upon exposure to light.<sup>66</sup> This strategy used a desktop printer to pattern different color inks as hinges on a

homogeneous polystyrene sheet. Printed inks on the surface of polymer sheet absorb light on the basis of the wavelength of light and the color of the inks. The absorbed light heats the underlying polystyrene sheet resulting in folding due to strain relief. Different color inks that absorb differently at the same wavelength can be patterned on the same polymer sheet, providing sequential control of sheet folding with respect to time and space after light exposure.

Polymers for the biological interface: Advances in materials for AM offer the ability to reproduce the 3D complexity in biological systems. With the growing interest in personalized and patient-centered medical treatment, digital manufacturing can enable the transformation of medical image files from CT scans and MRI to provide blueprints for the construction of tissue, organ models, or surgical guides.<sup>67,68</sup>

Bioprinting is a subset of AM that involves the deposition of biomaterials, biochemicals, and living cells with spatial control to

fabricate 3D structures that can recapitulate biological function.<sup>68</sup> Bioprinting with natural polysaccharides, proteins, or a combination of the two thereof have resulted in a number of promising reports for tissue engineering and regenerative medicine. AM processes based on inkjet printing, material extrusion, and laser deposition are the most common methodologies for the deposition of these biomaterials.<sup>69–71</sup>

**Biomaterials for material extrusion printing:** In general, bioinks have some of the same requirements as abiotic materials (printability, resolution, structural integrity, and mechanical properties), but also require other points of consideration such as cell viability and proliferation, biocompatibility, biodegradation and remodeling, and immune response. Most biological environments are aqueous, and thus, hydrogels are commonly employed as the printed matrix. The viscoelastic behavior of the biomaterials before, during, and after printing are of utmost importance for all bioprinting strategies.<sup>71</sup> The most common biomaterials that have been optimized for bioprinting are gelatin methacrylate, alginate, hyaluronic acid, and PEG-based materials. However, these materials can be limited in the tunability of their physicochemical properties. Thus, there are opportunities to develop new polymeric biomaterials beyond these ubiquitously used biomaterials.

Hybrid strategies that merge our understanding of molecular and supramolecular chemistry with natural biopolymers can afford versatile bioink platforms. Methacrylation is a common approach<sup>51,72,73</sup> to afford biopolymers that can undergo chemical cross-linking in the presence of a photoradical generator, although more elegant strategies have also emerged. For example, Burdick and co-workers employed the host–guest chemistry between adamantyl and  $\beta$ -cyclodextrin groups appended onto separate hyaluronic acid chains (Ad-HA and CD-HA, respectively) (Figure 6a[i]).<sup>74</sup> Aqueous mixtures of these polymers afforded shear-thinning and self-healing hydrogels that was utilized as both the extrudable ink and the support gel into which the ink was extruded (Figure 6a[ii,iii]). Biocompatible 3D constructs were printed with high resolution, and the bioink was covalently cross-linked by polymerizing methacrylated hyaluronic acid. Additionally, the surrounding support gel could be washed away afterward due to the reversibility of the host–guest interaction (Figure 6a[iii]).

Despite the advances in this field, there are still several challenges that remain. (i) The biochemical cues for tissues can be complex and even dynamic. 3D printed hydrogels for tissue engineering must promote basic cell processes including adhesion, proliferation, and differentiation. Recent developments in bioprinting tissue-derived decellularized extracellular matrices (dECM) could help to address this limitation.<sup>75,76</sup> (ii) Another challenge is to achieve high cell density as observed in native tissue. A minimum concentration of polymer or biopolymer is required for printability and mechanical properties, but the material occupies a volume of space within the hydrogel that limits the volume in which the cells can reside. A decrease in the polymer or biopolymer concentration results in soft hydrogels that lose their printability because they are not self-supporting. An alternative strategy has been pioneered by Feinberg and co-workers known as freeform reversible embedding of suspended hydrogels (FRESH) printing. This process improves the print fidelity of soft hydrogel constructs by depositing and embedding the printed hydrogel directly into a second hydrogel support bath comprised of gelatin. Biomaterials with low elastic moduli (<500 kPa) can be printed using this approach and are applicable to a broad range of biopolymers

(alginate, collagen, and fibrin).<sup>77</sup> Feinberg and co-workers also demonstrated 3D printing of hydrophobic polydimethylsiloxane (PDMS) prepolymer in a hydrophilic Carbopol gel support.<sup>78</sup> 3D printed PDMS helix, tube, helical tube, and bifurcation with a webbed fork were successfully obtained using this strategy. (Figure 6b). Russel and co-workers reported liquid-in-liquid printing using jammed nanoparticles at liquid–liquid interfaces. This form of printing can afford dynamic and soft liquid materials for the encapsulation of cells or as stimuli-responsive materials that could be suitable for biological interfaces.<sup>79,80</sup> (iii) Lastly, the degradation of the biopolymer matrix needs to be synchronized with cell growth and the generation of new ECM. Polymers that are degradable or easily remodeled by the encapsulated cells would be ideal for this purpose.

**Biomaterials for vat photopolymerization printing:** Vat photopolymerization processes (laser-scanning SLA or DLP SLA) offer precise and rapid manufacturing for 3D biofabrication. Light-based methods can offer a higher resolution and the fabrication of more complex geometries relative to extrusion-based bioprinting methods. A particular challenge is to create vascularized tissue wherein multivascular networks are formed within a biocompatible hydrogel.<sup>81</sup> Currently, vat photopolymerization for biofabrication is limited to homogeneous objects printed from a singular resin. The next generation of polymer and engineering advances could include multimaterial light-based processes for printing biological structures.

**Sustainability in AM:** The future of AM as an advanced form of manufacturing should rely on sustainable sources of resins and inks, as well as pathways for polymer recycling, upcycling, and chemical circularity. Poly(lactic acid) (PLA) is a popular filament for FDM printing. PLA can be sustainably sourced and is compostable, but is limited in its use as a commodity plastic by its thermal and mechanical stability. The polymer community has an opportunity to redefine the types of materials that are developed as plastics and the advanced manufacturing technologies required for processing these materials. Sustainably sourced compounds can provide an alternative to petroleum-based products that are used today;<sup>82,83</sup> some examples include naturally occurring compounds such as eugenol (derived from lignin)<sup>84</sup> and terpenes (isolated from plants).<sup>85</sup> The Dove group has shown that thiol–ene click chemistry can be used in a vat photopolymerization process to create poly(terpenoid) objects. The tunability of the mechanical properties and surface properties demonstrate the utility of this approach for future applications. In addition, Voet and co-workers have developed biobased photopolymer resins based on modified soybean oil for SLA printing.<sup>86</sup> Soybean oil methacrylates were synthesized from epoxidized soybean oil resulting in products with dimethacrylates or trimethacrylates. A library of photoresins with up to 80% of soybean oil (meth)acrylates, monofunctional diluents, and photoinitiators was generated to achieve a maximum biobased content and a low viscosity for 3D printing applications. The 3D printed parts with complete layer fusion and accurate print quality were obtained.

The future of additive manufacturing will depend on new polymeric materials that are specifically designed for these technologies. The recent advances in AM hardware, software, and modeling will require polymers that are (1) developed based on the processing requirements of the printing technology and (2) afford the physicochemical properties desired of the final printed object. At the present, AM is expected to impact the aerospace and automobile markets with printed parts, and the healthcare space with personalized surgical guides, dental molds,

prosthetics, and hearing aids. With the recent global Coronavirus pandemic, we have already seen the emergence of AM for the distributed production of personal protective equipment, such as face shields, which are in short supply. Moving forward, there is a tremendous opportunity for new materials to forge new paths toward applications that previously were never considered because this technology was unavailable. Fundamental advancements in polymer science will continue to drive and create these possibilities. New chemistries for AM processes, integration of polymer architectures into AM resin design, stimuli-responsive materials for AM, novel biomaterials, and sustainability comprise the essential elements for the progression of AM as a technology. It is too soon to understand the full scope of AM in future manufacturing processes, but the potential opportunities warrant the excitement that we have seen in the field.

## ■ AUTHOR INFORMATION

### Corresponding Author

Alshakim Nelson — The Department of Chemistry, University of Washington, Seattle, Washington 98195, United States;  
✉ orcid.org/0000-0001-8060-8611; Email: [alshakim@uw.edu](mailto:alshakim@uw.edu)

Complete contact information is available at:  
<https://pubs.acs.org/10.1021/acsmacrollett.0c00200>

### Notes

The authors declare no competing financial interest.

## ■ ACKNOWLEDGMENTS

We gratefully acknowledge support from the National Science Foundation (1752972) and the U.S. Army Research Office (W911NF-17-1-0595). B.N. thanks the Dalton Postdoctoral Fellowship.

## ■ REFERENCES

- (1) Staudinger, H. Über Polymerisation. *Ber. Dtsch. Chem. Ges.* **1920**, *53*, 1073–1085.
- (2) Hofmann, M. 3D Printing Gets a Boost and Opportunities with Polymer Materials. *ACS Macro Lett.* **2014**, *3*, 382–386.
- (3) Ligon, S. C.; Liska, R.; Stampfl, J.; Gurr, M.; Mülhaupt, R. Polymers for 3D Printing and Customized Additive Manufacturing. *Chem. Rev.* **2017**, *117*, 10212–10290.
- (4) Hribar, K. C.; Soman, P.; Warner, J.; Chung, P.; Chen, S. Light-Assisted Direct-Write of 3D Functional Biomaterials. *Lab Chip* **2014**, *14*, 268–275.
- (5) Jose, R. R.; Rodriguez, M. J.; Dixon, T. A.; Omenetto, F.; Kaplan, D. L. Evolution of Bioinks and Additive Manufacturing Technologies for 3D Bioprinting. *ACS Biomater. Sci. Eng.* **2016**, *2*, 1662–1678.
- (6) Boydston, A. J.; Cao, B.; Nelson, A.; Ono, R. J.; Saha, A.; Schwartz, J. J.; Thrasher, C. J. Additive Manufacturing with Stimuli-Responsive Materials. *J. Mater. Chem. A* **2018**, *6*, 20621–20645.
- (7) Shafranek, R. T.; Millik, S. C.; Smith, P. T.; Lee, C.-U.; Boydston, A. J.; Nelson, A. Stimuli-Responsive Materials in Additive Manufacturing. *Prog. Polym. Sci.* **2019**, *93*, 36–67.
- (8) Chatham, C. A.; Long, T. E.; Williams, C. B. A Review of the Process Physics and Material Screening Methods for Polymer Powder Bed Fusion Additive Manufacturing. *Prog. Polym. Sci.* **2019**, *93*, 68–95.
- (9) Appuhamilage, G. A.; Chartrain, N.; Meenakshisundaram, V.; Feller, K. D.; Williams, C. B.; Long, T. E. 110th Anniversary: Vat Photopolymerization-Based Additive Manufacturing: Current Trends and Future Directions in Materials Design. *Ind. Eng. Chem. Res.* **2019**, *58*, 15109–15118.
- (10) Bagheri, A.; Jin, J. Photopolymerization in 3D Printing. *ACS Appl. Polym. Mater.* **2019**, *1*, 593–611.
- (11) Chatani, S.; Kloxin, C. J.; Bowman, C. N. The Power of Light in Polymer Science: Photochemical Processes to Manipulate Polymer Formation, Structure, and Properties. *Polym. Chem.* **2014**, *5*, 2187–2201.
- (12) Compton, B. G.; Lewis, J. A. 3D-Printing of Lightweight Cellular Composites. *Adv. Mater.* **2014**, *26*, 5930–5935.
- (13) Lin, S.; Liu, J.; Liu, X.; Zhao, X. Muscle-like Fatigue-Resistant Hydrogels by Mechanical Training. *Proc. Natl. Acad. Sci. U. S. A.* **2019**, *116*, 10244–10249.
- (14) Wong, J.; Gong, A. T.; Defnet, P. A.; Meabe, L.; Beauchamp, B.; Sweet, R. M.; Sardon, H.; Cobb, C. L.; Nelson, A. 3D Printing Ionogel Auxetic Frameworks for Stretchable Sensors. *Adv. Mater. Technol.* **2019**, *4*, 1900452.
- (15) Wu, A. S.; Small IV, W.; Bryson, T. M.; Cheng, E.; Metz, T. R.; Schulze, S. E.; Duoss, E. B.; Wilson, T. S. 3D Printed Silicones with Shape Memory. *Sci. Rep.* **2017**, *7*, 4664.
- (16) Valino, A. D.; Dizon, J. R. C.; Espera, A. H.; Chen, Q.; Messman, J.; Advincula, R. C. Advances in 3D Printing of Thermoplastic Polymer Composites and Nanocomposites. *Prog. Polym. Sci.* **2019**, *98*, 101162.
- (17) Li, L.; Zhang, P.; Zhang, Z.; Lin, Q.; Wu, Y.; Cheng, A.; Lin, Y.; Thompson, C. M.; Smaldone, R. A.; Ke, C. Hierarchical Co-Assembly Enhanced Direct Ink Writing. *Angew. Chem.* **2018**, *130*, 5199–5203.
- (18) Kim, Y.; Yuk, H.; Zhao, R.; Chester, S. A.; Zhao, X. Printing Ferromagnetic Domains for Untethered Fast-Transforming Soft Materials. *Nature* **2018**, *558*, 274–279.
- (19) Skylar-Scott, M. A.; Mueller, J.; Visser, C. W.; Lewis, J. A. Voxelated Soft Matter via Multimaterial Multinozzle 3D Printing. *Nature* **2019**, *575*, 330–335.
- (20) Hardin, J. O.; Ober, T. J.; Valentine, A. D.; Lewis, J. A. Microfluidic Printheads for Multimaterial 3D Printing of Viscoelastic Inks. *Adv. Mater.* **2015**, *27*, 3279–3284.
- (21) Smith, P. T.; Basu, A.; Saha, A.; Nelson, A. Chemical Modification and Printability of Shear-Thinning Hydrogel Inks for Direct-Write 3D Printing. *Polymer* **2018**, *152*, 42–50.
- (22) Paxton, N.; Smolan, W.; Böck, T.; Melchels, F.; Groll, J.; Jungst, T. Proposal to Assess Printability of Bioinks for Extrusion-Based Bioprinting and Evaluation of Rheological Properties Governing Bioprintability. *Biofabrication* **2017**, *9*, 44107.
- (23) Nadgorny, M.; Xiao, Z.; Connal, L. A. 2D and 3D-Printing of Self-Healing Gels: Design and Extrusion of Self-Rolling Objects. *Mol. Syst. Des. Eng.* **2017**, *2*, 283–292.
- (24) Davidson, J. R.; Appuhamilage, G. A.; Thompson, C. M.; Voit, W.; Smaldone, R. A. Design Paradigm Utilizing Reversible Diels–Alder Reactions to Enhance the Mechanical Properties of 3D Printed Materials. *ACS Appl. Mater. Interfaces* **2016**, *8*, 16961–16966.
- (25) Tumbleston, J. R.; Shirvanyants, D.; Ermoshkin, N.; Januszewicz, R.; Johnson, A. R.; Kelly, D.; Chen, K.; Pischmidt, R.; Rolland, J. P.; Ermoshkin, A.; Samulski, E. T.; DeSimone, J. M. Continuous Liquid Interface Production of 3D Objects. *Science* **2015**, *347*, 1349–1352.
- (26) de Beer, M. P.; van der Laan, H. L.; Cole, M. A.; Whelan, R. J.; Burns, M. A.; Scott, T. F. Rapid, Continuous Additive Manufacturing by Volumetric Polymerization Inhibition Patterning. *Sci. Adv.* **2019**, *5*, eaau8723–eaau8723.
- (27) Robertson, I. D.; Yourdkhani, M.; Centellas, P. J.; Aw, J. E.; Ivanoff, D. G.; Goli, E.; Lloyd, E. M.; Dean, L. M.; Sottos, N. R.; Geubelle, P. H.; Moore, J. S.; White, S. R. Rapid Energy-Efficient Manufacturing of Polymers and Composites via Frontal Polymerization. *Nature* **2018**, *557*, 223–227.
- (28) Valentin, T. M.; Leggett, S. E.; Chen, P.-Y.; Sodhi, J. K.; Stephens, L. H.; McClintock, H. D.; Sim, J. Y.; Wong, I. Y. Stereolithographic Printing of Ionically Crosslinked Alginate Hydrogels for Degradable Biomaterials and Microfluidics. *Lab Chip* **2017**, *17*, 3474–3488.
- (29) Zhang, Z.; Corrigan, N.; Bagheri, A.; Jin, J.; Boyer, C. A Versatile 3D and 4D Printing System through Photocrosslinked RAFT Polymerization. *Angew. Chem., Int. Ed.* **2019**, *58*, 17954–17963.
- (30) Warner, J. J.; Wang, P.; Mellor, W. M.; Hwang, H. H.; Park, J. H.; Pyo, S.-H.; Chen, S. 3D Printable Non-Isocyanate Polyurethanes with Tunable Material Properties. *Polym. Chem.* **2019**, *10*, 4665–4674.

(31) Kumar, S.; Hofmann, M.; Steinmann, B.; Foster, E. J.; Weder, C. Reinforcement of Stereolithographic Resins for Rapid Prototyping with Cellulose Nanocrystals. *ACS Appl. Mater. Interfaces* **2012**, *4*, 5399–5407.

(32) Palaganas, N. B.; Mangadlao, J. D.; de Leon, A. C. C.; Palaganas, J. O.; Pangilinan, K. D.; Lee, Y. J.; Advincula, R. C. 3D Printing of Photocurable Cellulose Nanocrystal Composite for Fabrication of Complex Architectures via Stereolithography. *ACS Appl. Mater. Interfaces* **2017**, *9*, 34314–34324.

(33) Schultz, A. R.; Lambert, P. M.; Chartrain, N. A.; Ruohoniemi, D. M.; Zhang, Z.; Jang, C.; Zhang, M.; Williams, C. B.; Long, T. E. 3D Printing Phosphonium Ionic Liquid Networks with Mask Projection Microstereolithography. *ACS Macro Lett.* **2014**, *3*, 1205–1209.

(34) Zawaski, C. E.; Wilts, E. M.; Chatham, C. A.; Stevenson, A. T.; Pekkanen, A. M.; Li, C.; Tian, Z.; Whittington, A. R.; Long, T. E.; Williams, C. B. Tuning the Material Properties of a Water-Soluble Ionic Polymer Using Different Counterions for Material Extrusion Additive Manufacturing. *Polymer* **2019**, *176*, 283–292.

(35) Wales, D. J.; Cao, Q.; Kastner, K.; Karjalainen, E.; Newton, G. N.; Sans, V. 3D-Printable Photochromic Molecular Materials for Reversible Information Storage. *Adv. Mater.* **2018**, *30*, 1800159.

(36) Maciel, V. G.; Wales, D. J.; Seferin, M.; Sans, V. Environmental Performance of 3D-Printing Polymerisable Ionic Liquids. *J. Cleaner Prod.* **2019**, *214*, 29–40.

(37) Li, X.; Yu, R.; He, Y.; Zhang, Y.; Yang, X.; Zhao, X.; Huang, W. Self-Healing Polyurethane Elastomers Based on a Disulfide Bond by Digital Light Processing 3D Printing. *ACS Macro Lett.* **2019**, *8*, 1511–1516.

(38) Hegde, M.; Meenakshisundaram, V.; Chartrain, N.; Sekhar, S.; Tafti, D.; Williams, C. B.; Long, T. E. 3D Printing All-Aromatic Polyimides Using Mask-Projection Stereolithography: Processing the Nonprocessable. *Adv. Mater.* **2017**, *29*, 1701240.

(39) Peterson, G. I.; Schwartz, J. J.; Zhang, D.; Weiss, B. M.; Ganter, M. A.; Storti, D. W.; Boydston, A. J. Production of Materials with Spatially-Controlled Cross-Link Density via Vat Photopolymerization. *ACS Appl. Mater. Interfaces* **2016**, *8*, 29037–29043.

(40) Dolinski, N. D.; Page, Z. A.; Callaway, E. B.; Eisenreich, F.; Garcia, R. V.; Chavez, R.; Bothman, D. P.; Hecht, S.; Zok, F. W.; Hawker, C. J. Solution Mask Liquid Lithography (SMaLL) for One-Step, Multimaterial 3D Printing. *Adv. Mater.* **2018**, *30*, 1800364.

(41) Schwartz, J. J.; Boydston, A. J. Multimaterial Actinic Spatial Control 3D and 4D Printing. *Nat. Commun.* **2019**, *10*, 791.

(42) Müller, M.; Becher, J.; Schnabelrauch, M.; Zenobi-Wong, M. Nanostructured Pluronic Hydrogels as Bioinks for 3D Bioprinting. *Biofabrication* **2015**, *7*, 35006.

(43) Zhang, M.; Vora, A.; Han, W.; Wojtecki, R. J.; Maune, H.; Le, A. B. A.; Thompson, L. E.; McClelland, G. M.; Ribet, F.; Engler, A. C.; Nelson, A. Dual-Responsive Hydrogels for Direct-Write 3D Printing. *Macromolecules* **2015**, *48*, 6482–6488.

(44) Karis, D. G.; Ono, R. J.; Zhang, M.; Vora, A.; Storti, D.; Ganter, M. A.; Nelson, A. Cross-Linkable Multi-Stimuli Responsive Hydrogel Inks for Direct-Write 3D Printing. *Polym. Chem.* **2017**, *8*, 4199–4206.

(45) Murphy, R.; Walsh, D. P.; Hamilton, C. A.; Cryan, S.-A.; het Panhuis, M.; Heise, A. Degradable 3D-Printed Hydrogels Based on Star-Shaped Copolypeptides. *Biomacromolecules* **2018**, *19*, 2691–2699.

(46) Lin, Q.; Li, L.; Tang, M.; Hou, X.; Ke, C. Rapid Macroscale Shape Morphing of 3D-Printed Polyrotaxane Monoliths Amplified from PH-Controlled Nanoscale Ring Motions. *J. Mater. Chem. C* **2018**, *6*, 11956–11960.

(47) Lin, Q.; Li, L.; Tang, M.; Hou, X.; Ke, C. Rapid Macroscale Shape Morphing of 3D-Printed Polyrotaxane Monoliths Amplified from PH-Controlled Nanoscale Ring Motions. *J. Mater. Chem. C* **2018**, *6*, 11956–11960.

(48) Mondschein, R. J.; Kanitkar, A.; Williams, C. B.; Verbridge, S. S.; Long, T. E. Polymer Structure-Property Requirements for Stereolithographic 3D Printing of Soft Tissue Engineering Scaffolds. *Biomaterials* **2017**, *140*, 170–188.

(49) Schüller-Ravoo, S.; Teixeira, S. M.; Feijen, J.; Grijpma, D. W.; Poot, A. A. Flexible and Elastic Scaffolds for Cartilage Tissue Engineering Prepared by Stereolithography Using Poly(Trimethylene Carbonate)-Based Resins. *Macromol. Biosci.* **2013**, *13*, 1711–1719.

(50) Le Fer, G.; Luo, Y.; Becker, M. L. Poly(Propylene Fumarate) Stars, Using Architecture to Reduce the Viscosity of 3D Printable Resins. *Polym. Chem.* **2019**, *10*, 4655–4664.

(51) Smith, P. T.; Narupai, B.; Tsui, J. H.; Millik, S. C.; Shafranek, R. T.; Kim, D.-H.; Nelson, A. Additive Manufacturing of Bovine Serum Albumin-Based Hydrogels and Bioplastics. *Biomacromolecules* **2020**, *21*, 484–492.

(52) Truby, R. L.; Lewis, J. A. Printing Soft Matter in Three Dimensions. *Nature* **2016**, *540*, 371–378.

(53) Sydney Gladman, A.; Matsumoto, E. A.; Nuzzo, R. G.; Mahadevan, L.; Lewis, J. A. Biomimetic 4D Printing. *Nat. Mater.* **2016**, *15*, 413–418.

(54) Wu, C.; Wang, X. Globule-to-Coil Transition of a Single Homopolymer Chain in Solution. *Phys. Rev. Lett.* **1998**, *80*, 4092–4094.

(55) Bakarich, S. E.; Gorkin, R.; Panhuis, M. i. h.; Spinks, G. M. 4D Printing with Mechanically Robust, Thermally Actuating Hydrogels. *Macromol. Rapid Commun.* **2015**, *36*, 1211–1217.

(56) Han, D.; Lu, Z.; Chester, S. A.; Lee, H. Micro 3D Printing of a Temperature-Responsive Hydrogel Using Projection Micro-Stereolithography. *Sci. Rep.* **2018**, *8*, 1963.

(57) Dutta, S.; Cohn, D. Temperature and PH Responsive 3D Printed Scaffolds. *J. Mater. Chem. B* **2017**, *5*, 9514–9521.

(58) Peterson, G. I.; Larsen, M. B.; Ganter, M. A.; Storti, D. W.; Boydston, A. J. 3D-Printed Mechanochromic Materials. *ACS Appl. Mater. Interfaces* **2015**, *7*, 577–583.

(59) Cao, B.; Boechler, N.; Boydston, A. J. Additive Manufacturing with a Flex Activated Mechanophore for Nondestructive Assessment of Mechanochemical Reactivity in Complex Object Geometries. *Polymer* **2018**, *152*, 4–8.

(60) Rohde, R. C.; Basu, A.; Okello, L. B.; Barbee, M. H.; Zhang, Y.; Velev, O. D.; Nelson, A.; Craig, S. L. Mechanochromic Composite Elastomers for Additive Manufacturing and Low Strain Mechanophore Activation. *Polym. Chem.* **2019**, *10*, 5985–5991.

(61) Kuang, X.; Roach, D. J.; Wu, J.; Hamel, C. M.; Ding, Z.; Wang, T.; Dunn, M. L.; Qi, H. J. Advances in 4D Printing: Materials and Applications. *Adv. Funct. Mater.* **2019**, *29*, 1805290.

(62) Zhang, Z.; Demir, K. G.; Gu, G. X. Developments in 4D-Printing: A Review on Current Smart Materials, Technologies, and Applications. *Int. J. Smart Nano Mater.* **2019**, *10*, 205–224.

(63) Momeni, F.; M. Mehdi Hassani, N. S.; Liu, X.; Ni, J. A Review of 4D Printing. *Mater. Des.* **2017**, *122*, 42–79.

(64) Kotikian, A.; Truby, R. L.; Boley, J. W.; White, T. J.; Lewis, J. A. 3D Printing of Liquid Crystal Elastomeric Actuators with Spatially Programmed Nematic Order. *Adv. Mater.* **2018**, *30*, 1706164.

(65) Boyle, B. M.; French, T. A.; Pearson, R. M.; McCarthy, B. G.; Miyake, G. M. Structural Color for Additive Manufacturing: 3D-Printed Photonic Crystals from Block Copolymers. *ACS Nano* **2017**, *11*, 3052–3058.

(66) Liu, Y.; Shaw, B.; Dickey, M. D.; Genzer, J. Sequential Self-Folding of Polymer Sheets. *Sci. Adv.* **2017**, *3*, No. e1602417.

(67) Qiu, K.; Haghiashtiani, G.; McAlpine, M. C. 3D Printed Organ Models for Surgical Applications. *Annu. Rev. Anal. Chem.* **2018**, *11*, 287–306.

(68) Murphy, S. V.; Atala, A. 3D Bioprinting of Tissues and Organs. *Nat. Biotechnol.* **2014**, *32*, 773–785.

(69) Tasoglu, S.; Demirci, U. Bioprinting for Stem Cell Research. *Trends Biotechnol.* **2013**, *31*, 10–19.

(70) Zhang, Y. S.; Yue, K.; Aleman, J.; Mollazadeh-Moghaddam, K.; Bakht, S. M.; Yang, J.; Jia, W.; Dell'Erba, V.; Assawes, P.; Shin, S. R.; Dokmeci, M. R.; Oklu, R.; Khademhosseini, A. 3D Bioprinting for Tissue and Organ Fabrication. *Ann. Biomed. Eng.* **2017**, *45*, 148–163.

(71) Hospoduk, M.; Dey, M.; Sosnoski, D.; Ozbolat, I. T. The Bioink: A Comprehensive Review on Bioprintable Materials. *Biotechnol. Adv.* **2017**, *35*, 217–239.

(72) Shirahama, H.; Lee, B. H.; Tan, L. P.; Cho, N.-J. Precise Tuning of Facile One-Pot Gelatin Methacryloyl (GelMA) Synthesis. *Sci. Rep.* **2016**, *6*, 31036.

(73) Kesti, M.; Müller, M.; Becher, J.; Schnabelrauch, M.; D'Este, M.; Eglin, D.; Zenobi-Wong, M. A Versatile Bioink for Three-Dimensional Printing of Cellular Scaffolds Based on Thermally and Photo-Triggered Tandem Gelation. *Acta Biomater.* **2015**, *11*, 162–172.

(74) Highley, C. B.; Rodell, C. B.; Burdick, J. A. Direct 3D Printing of Shear-Thinning Hydrogels into Self-Healing Hydrogels. *Adv. Mater.* **2015**, *27*, 5075–5079.

(75) Ma, X.; Yu, C.; Wang, P.; Xu, W.; Wan, X.; Lai, C. S. E.; Liu, J.; Koroleva-Maharajh, A.; Chen, S. Rapid 3D Bioprinting of Decellularized Extracellular Matrix with Regionally Varied Mechanical Properties and Biomimetic Microarchitecture. *Biomaterials* **2018**, *185*, 310–321.

(76) Yu, C.; Ma, X.; Zhu, W.; Wang, P.; Miller, K. L.; Stupin, J.; Koroleva-Maharajh, A.; Hairabedian, A.; Chen, S. Scanningless and Continuous 3D Bioprinting of Human Tissues with Decellularized Extracellular Matrix. *Biomaterials* **2019**, *194*, 1–13.

(77) Hinton, T. J.; Jallerat, Q.; Palchesko, R. N.; Park, J. H.; Grodzicki, M. S.; Shue, H.-J.; Ramadan, M. H.; Hudson, A. R.; Feinberg, A. W. Three-Dimensional Printing of Complex Biological Structures by Freeform Reversible Embedding of Suspended Hydrogels. *Sci. Adv.* **2015**, *1*, No. e1500758.

(78) Hinton, T. J.; Hudson, A.; Pusch, K.; Lee, A.; Feinberg, A. W. 3D Printing PDMS Elastomer in a Hydrophilic Support Bath via Freeform Reversible Embedding. *ACS Biomater. Sci. Eng.* **2016**, *2*, 1781–1786.

(79) Forth, J.; Liu, X.; Hasnain, J.; Toor, A.; Miszta, K.; Shi, S.; Geissler, P. L.; Emrick, T.; Helms, B. A.; Russell, T. P. Reconfigurable Printed Liquids. *Adv. Mater.* **2018**, *30*, 1707603.

(80) Cui, M.; Emrick, T.; Russell, T. P. Stabilizing Liquid Drops in Nonequilibrium Shapes by the Interfacial Jamming of Nanoparticles. *Science* **2013**, *342*, 460–463.

(81) Grigoryan, B.; Paulsen, S. J.; Corbett, D. C.; Sazer, D. W.; Fortin, C. L.; Zaita, A. J.; Greenfield, P. T.; Calafat, N. J.; Gounley, J. P.; Ta, A. H.; Johansson, F.; Randles, A.; Rosenkrantz, J. E.; Louis-Rosenberg, J. D.; Galie, P. A.; Stevens, K. R.; Miller, J. S. Multivascular Networks and Functional Intravascular Topologies within Biocompatible Hydrogels. *Science* **2019**, *364*, 458–464.

(82) Nicastro, K. H.; Kloxin, C. J.; Epps, T. H. Potential Lignin-Derived Alternatives to Bisphenol A in Diamine-Hardened Epoxy Resins. *ACS Sustainable Chem. Eng.* **2018**, *6*, 14812–14819.

(83) Emerson, J. A.; Garabedian, N. T.; Burris, D. L.; Furst, E. M.; Epps, T. H. Exploiting Feedstock Diversity To Tune the Chemical and Tribological Properties of Lignin-Inspired Polymer Coatings. *ACS Sustainable Chem. Eng.* **2018**, *6*, 6856–6866.

(84) Ding, R.; Du, Y.; Goncalves, R. B.; Francis, L. F.; Reineke, T. M. Sustainable near UV-Curable Acrylates Based on Natural Phenolics for Stereolithography 3D Printing. *Polym. Chem.* **2019**, *10*, 1067–1077.

(85) Weems, A. C.; Delle Chiaie, K. R.; Yee, R.; Dove, A. P. Selective Reactivity of Myrcene for Vat Photopolymerization 3D Printing and Postfabrication Surface Modification. *Biomacromolecules* **2020**, *21*, 163–170.

(86) Guit, J.; Tavares, M. B. L.; Hul, J.; Ye, C.; Loos, K.; Jager, J.; Folkersma, R.; Voet, V. S. D. Photopolymer Resins with Biobased Methacrylates Based on Soybean Oil for Stereolithography. *ACS Appl. Polym. Mater.* **2020**, *2*, 949–957.